

# Biogenic Silver Nanoparticles as Sensors of $\text{Cu}^{2+}$ and $\text{Pb}^{2+}$ in Aqueous Solutions

Luisa E. Silva-De Hoyos<sup>1,2</sup>, Victor Sánchez-Mendieta<sup>1,\*</sup>, Alfredo R. Vilchis-Nestor<sup>2</sup>, Miguel A. Camacho-López<sup>3</sup>

<sup>1</sup>Faculty of Chemistry, Autonomous University of the State of Mexico, Mexico

<sup>2</sup>Center for Research in Sustainable Chemistry, Autonomous University of the State of Mexico, Mexico

<sup>3</sup>Laboratory of Photomedicine, Biophotonics and Ultra-short Pulse Laser Spectroscopy, Faculty of Medicine, Autonomous University of the State of Mexico, Mexico

Copyright©2017 by authors, all rights reserved. Authors agree that this article remains permanently open access under the terms of the Creative Commons Attribution License 4.0 International License

**Abstract** Silver nanoparticles (Ag-NPs) were bio-synthesized using *Camellia sinensis* (green tea) aqueous extract. Nanoparticles prepared with  $10^{-3}$  M  $\text{AgNO}_3$  solution, using 3mL of green tea extract and at  $60^\circ\text{C}$ , have spherical shape with a mean diameter of 7nm. The formation of the nanoparticles was confirmed by UV-Vis spectrophotometry through studies of the surface plasmon resonance (SPR). The morphology, size and crystalline structure of the Ag-NPs were determined using high definition transmission electron microscopy (TEM). Moreover, these green synthesized Ag-NPs were found to exhibit good sensing properties towards  $\text{Cu}^{2+}$  and  $\text{Pb}^{2+}$  ions in aqueous solutions. This metal ions-sensing ability of the biogenic Ag-NPs was monitored by UV-Vis spectrophotometry (SPR analyses) and fluorescence spectroscopy.

**Keywords** Biogenic-silver Nanoparticles, *Camellia Sinensis*, Nanoparticles Ion-sensing, Surface Plasmon Resonance Fluorescence

## 1. Introduction

Nowadays, nanotechnology has immense potential applications and is one of the most active areas of study [1-3]. Nanoparticles have drawn huge attention because of their great valuable properties on optical, electronic, medical, catalytic and sensor applications [4-7]. Noble-metal nanoparticles and their synthesis is an active area of academic research because of their forthcoming applications. There are, mainly, two ways of synthesis: chemical methods [8] and physical techniques [9]. Nevertheless, two of these methods have many problems such as the use of toxic solvents, generation of hazardous products and/or are not suitable to scale-up, among others. It is necessary to avoid adverse effects during synthesis and applications of nanoparticles; therefore, the growing need to apply an

eco-friendly and sustainable method for the synthesis of nanomaterials [10-12] using the biological approach, [6,13] is growing as alternative to reach these goals. To overcome these ill effects in chemical methods, plant extracts have been used for the synthesis of metal nanoparticles, due to the dual nature of the biomass as a reducing as well as a stabilizing agent [12, 14-17]. *Camellia sinensis* extract is rich in polyphenolic compounds. These are epicatechin groups and other flavonols [18-20]. In the past few years, silver nanoparticles have attracted interest, due to their potential applications such as: biomedicine [21], as a disinfectant [22] and sensors (biosensors and naked-eyed) [23,24].

The detection and quantification of heavy metal ions is an important subject in recent days, the usual techniques adopted for the detection of these metals involve spectrophotometric methods, which employs chromoionophores and ICP analysis. The majority of chromoionophores available for the detection are soluble in organic solvents, which limit the day-to-day applications and pollute even more the environment [25-28]. It is desirable to find procedures for selective naked-eye detection of metal ions in aqueous media that do not require a specific instrumentation, especially for field-test [23]. Optical reports methodologies listed in the literature for the detection of metal ions are base the surface plasmon resonance of silver nanoparticles, due to dependence of the plasmon shift with the chemical environment surrounding the Ag nanoparticles [29-31]. Moreover, surface plasmon resonance applied to colorimetric sensors does not require a uniform size and shape of the nanoparticles [28].

In this work, biogenic silver nanoparticles (Ag-NPs) were synthesized assisted by *Camellia sinensis* aqueous extract as a reducing and capping agent. The resulting colloidal array is evaluated in the selective colorimetric, plasmonic and fluorescent detection of  $\text{Cu}^{2+}$  and  $\text{Pb}^{2+}$  ions in aqueous solutions.

## 2. Materials and Methods

### 2.1. Materials

*Camellia sinensis* tea was obtained from a local store. Silver nitrate ( $\text{AgNO}_3$ ), Rhodamine 6G (Rh6G), ammonia solution, copper chloride ( $\text{CuCl}_2$ ), lead chloride ( $\text{PbCl}_2$ ), were acquired as analytical grade reagents from Sigma-Aldrich and used without any further purification.

### 2.2 Preparation of *Camellia Sinensis* Extract

The content of one bag of commercial green tea (Lagg's) (1.338g) was boiled for 10min in 100mL of deionized water; upon cooling the infusion was vacuum-filtered. The resulting aqueous extract was stored during a day and used for further experiments as a bioreducing agent.

### 2.3. Biosynthesis of Ag-NPs

The biological synthesis of silver nanoparticles was carried out by using 5mL of a  $10^{-3}$ M silver nitrate solution, adding 2.5mL of an ammonia solution, heating to  $60^\circ\text{C}$  during 24h and then pouring 2, 3 or 4mL of *Camellia sinensis* aqueous extract, respectively. This synthesis is an adaptation of the method reported for us previously [18].

### 2.4. Characterization of Ag-NPs

UV-Vis spectroscopy was performed using a Lambda 650 Perkin-Elmer spectrophotometer. For transmission electron microscopy (TEM) analyses, the samples were prepared by placing drops of the mixture reaction over carbon-coated grids and allowing evaporation. TEM observations were performed on a JEOL 2100 microscope operated at accelerating voltage of 200kV with a  $\text{LaB}_6$  filament. For calculating the amount and shape of nanoparticles in one sample, approximately 400 nanoparticles per sample were taken into account.

### 2.5. Sensing Studies

Sensing studies were performed only with the silver nanoparticles prepared from 3 mL of reducing agent at  $60^\circ\text{C}$ . 1 mL of a  $10^{-3}$  M solution of  $\text{Cu}^{2+}$  or  $\text{Pb}^{2+}$  was added to 1 mL of the silver nanoparticles solution at room temperature. To investigate the sensitivity effect of the biogenic silver nanoparticles toward detection of  $\text{Pb}^{2+}$  and  $\text{Cu}^{2+}$  metal ions, different concentrations of  $10^{-3}$ ,  $10^{-4}$  and  $10^{-5}$  M were

added to the silver nanoparticles colloidal suspension. The sensing and selectivity of the metal ions by the silver nanoparticles solution were analyzed by UV-Vis using a Lambda 650 Perkin-Elmer spectrophotometer. The sensing effect was also analyzed with fluorescence spectroscopy; first, 1 mL of Rh6G ( $10^{-3}$  M) was gradually added to 1 mL of biogenic silver nanoparticles and stirred for 30min. Then, to this solution 1mL of  $10^{-3}$  M of  $\text{CuCl}_2$  and  $\text{PbCl}_2$  aqueous solutions were added. The sensing experiment was monitored by a Horiba Jobin-Ivon, FluoroMax-P spectrofluorometer.

## 3. Results and Discussion

### 3.1 Synthesis and UV-Vis Analysis of Ag-NPs

The synthesis of Ag-NPs was initiated once the *Camellia sinensis* extract was introduced into 5mL of  $\text{AgNO}_3$  aqueous solution at  $60^\circ\text{C}$ . Solution turned almost immediately from a pale yellow to a light brownish color, which corroborates the formation of silver nanoparticles. This color change happens because the biomolecules present in the *Camellia sinensis* extract reduce the Ag metal ions to generate nanoparticles [11,23,32]. The main biomolecules existing in *Camellia sinensis* that act as reducing and passivating agents are: protocatechuic, caffeic acid, vanillic acid, syringic acid, catechin, epicatechin and benzoic acid, in the following amounts: 22.67, 830.10, 61.17, 75.91, 18.30, 1087.02 and 319.78mg per100g of extract, respectively [18]. It has been reported that the hydroxyl moieties, such as the ones found in epicatechin and caffeic acid, are responsible for the reduction of metal nanoparticles, since the OH groups are oxidized to the corresponding quinone [23]. As it is known, the amount of total phenolics in the extract corresponds to the total reducing agent amount; for green tea, it has been determined that the total amount is 59.8mg/g [18], which would be similar to the total reducing agent amount in our experiments.

As a result, the excitation of the surface plasmon resonance (SPR) occurs when Ag-NPs are irradiated with visible light. In Figure 1a, peaks with maxima between 394-400nm can be observed, their broadness indicate the polydispersity of the nanoparticles obtained [4,5,33]. These nanoparticles exhibit unique, as well as tunable optical properties that deepen on their surface plasmon resonance, which depends on shape, size, chemical environment and distribution of the nanoparticles [33].

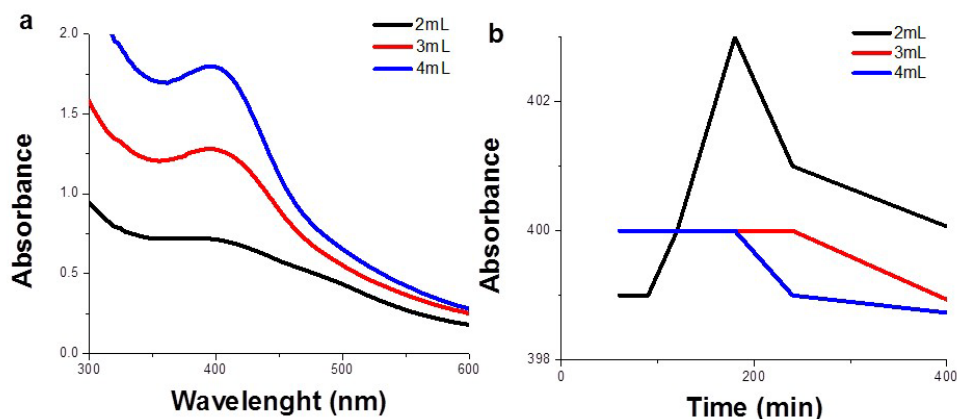


**Figure 1.** (a) UV-Vis spectra of biogenic Ag-NPs prepared at 60°C with 2, 3 and 4mL of reducing agent. (b) Plot of the intensity of the Surface Plasmon Resonance at 396nm of the Ag-NPs against the reaction time, obtained with different volumes of *Camellia sinensis* extract

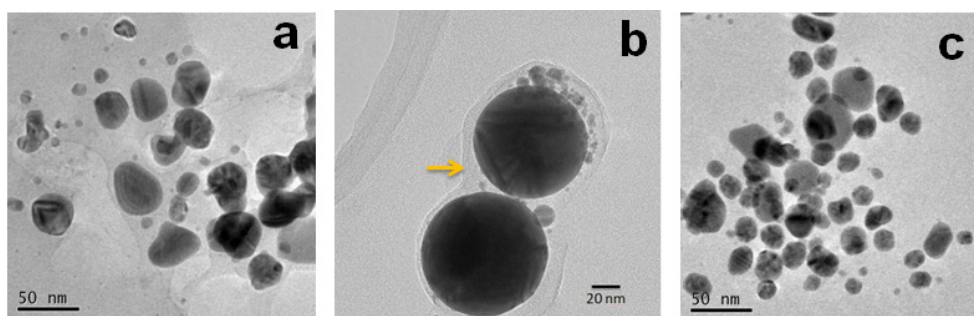


**Figure 2.** TEM images of biogenic Ag-NPs prepared at 60°C, with 2mL (a), 3mL (b) and 4mL (c) of reducing agent

The different amount of *Camellia sinensis* extract employed for the formation of Ag-NPs is reflected in the intensity, shape and wavelength position of the SPR peaks (Figure 1a). As less amount of reducing agent is used the more intense is the peak; on the contrary, when the concentration of reducing agent is increased a peak with less intensity is obtained. Since the intensity of the SPR signal is directly proportional to the amount of nanoparticles this means that less Ag-NPs are obtained. This can be explained by the possibility of agglomeration of Ag-NPs occurring when larger amount of *Camellia sinensis* extract is added to the Ag ions solution. Previous results have shown that excess concentration of metal ion precursor solution and/or higher concentration of reducing agent could lead to large quantities of nanoparticles with the final result of agglomeration of these [17,20], showing in UV-Vis studies as less intense and wider SPR signals. In addition, the red-shifting of the corresponding SPR peaks for the 3 and 4mL reducing agent formed Ag-NPs, compared to the profile of the curve related with 2mL of reducing agent Ag-NPs SPR peak, tells us that the morphology of these nanoparticles may be different. Figure 1b shows the plots of the absorbance at  $\lambda_{max}$  (396nm) for silver nanoparticles generated with different volumes of green tea extract. It can be seen that the SPR intensity at 400min decreases significantly, meaning the formation of bigger silver crystals due to the coalescence of nanoparticles after long periods of time. The Ag nanoparticles system is not stable in time as can be displayed by the behavior of the

plots in Figure 1b, then this can be attributable to close proximity of the nanoparticles and/or the poor efficiency of the biomolecules that act as capping agents, caused by intrinsic degradation process of biological molecules of the green tea extract. Nevertheless, this proximity of the nanoparticles, capped by biomolecules of the green tea, could create suitable moieties to attach to metal ions, modifying its chemical environment, therefore, sensing them with a good selectivity.

### 3.2. Morphology, Size and Crystalline Structure Analysis by TEM

The morphology, size distribution and crystal structure of the biosynthesized Ag-NPs were elucidated from the transmission electron microscopy (TEM) observations. Figure 2 shows the images of the Ag-NPs obtained.

Biogenic Ag-NPs with uneven sizes and average diameters between 10-40nm were obtained. Ag-NPs obtained with 2mL of *Camellia sinensis* extract have broader dispersion of size and morphology, as shown in Figure 2a. However, the increase in the amount of extract (3mL) resulted in a superior homogeneity of these nanoparticles, having spherical shape (Figure 2b). Though, for those Ag-NPs formed with 4mL of reducing agent, the particles lose some of their uniformity and have more spheroidal shapes (Figure 2c). It seems that the amount of the reducing

agent has an effect on the Ag-NPs morphology. It is important to mention that the layer of biomolecules present around each of the nanoparticles (Figure 2b) is related to the nanoparticle stability.

As can be seen in Figure 3, those nanoparticles obtained with 2mL of extract have a greater polydispersity with spherical, spheroidal and triangular shape with size range of 3 to 47nm (Figure 3a). In the case of the Ag-NPs obtained with 3mL of extract the shape is mostly spherical within a diameter range of 3 to 50nm (Figure 3b). And finally, the

Ag-NPs formed, using 4mL of extract, the shape tend to be spheroidal with a size range of 8 to 42nm (Figure 3c). The high resolution TEM images of the biogenic Ag-NPs, shown in Figure 3, demonstrate that the growth of these nanoparticles occurs preferentially on the (111) plane. In addition, the selected area diffraction (SAED) analysis yields the crystalline nature of the prepared nanoparticles and could be indexed to a FCC structure in all three cases (2, 3 and 4 mL of reducing agent added). The diffraction rings also suggested the NPs were polycrystalline.

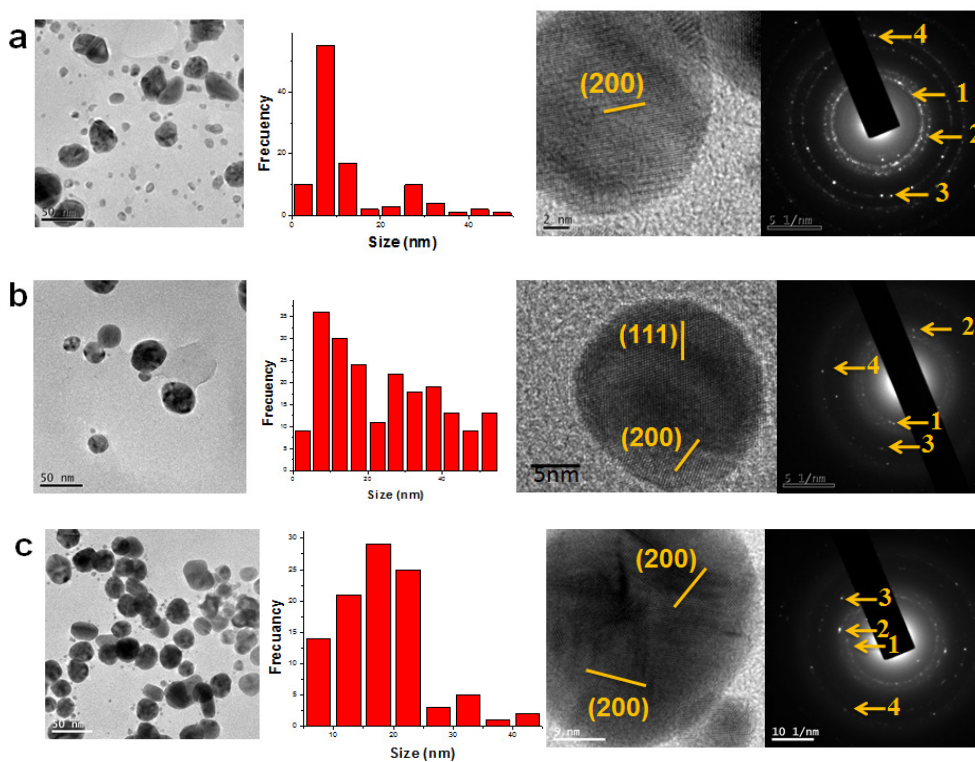


**Figure 3.** TEM images, histograms, HRTEM micrographs and selected area diffraction patterns of biogenic Ag-NPs obtained at 60°C with 2mL (a), 3mL (b) and 4mL (c) of reducing agent (*Camellia sinensis* extract). Selected area diffraction patterns of: Rings 1, 2, 3 correspond to {111}, {200}, {222}, {311} reflections (a). Rings 1, 2, 3 correspond to {111}, {200}, {222}, {311} (b) and Rings 1, 2, 3 correspond to {200}, {220}, {222}, {400}, family planes (c), respectively, corresponding to face-centered cubic (FCC) silver.

### 3.3. Metal Ions Sensing Studies

#### 3.3.1. Detection of Metal Ions

Based on the morphological properties of shape and size distribution, the biogenic Ag-NPs prepared at 60°C with 3mL of reducing agent were chosen for the sensing studies. It is important to mention that a pH of 5.01 was determined in the Ag-NPs solution previously to the interaction with the metal ions. Other similar studies have employed Ag nanoparticles solution of pH values around 5. This pH value allows that carboxylic moieties of the passivation agent could be in ionized form, which is important to enhance the electrostatic character of the nanoparticles surface. This promotes the interaction with the metal ions to probe.

Figure 4 exhibits UV-Vis absorption studies at different times of the Ag-NPs that were used as sensors; this sample presents surface plasmon resonance signals centered at 400nm from 60 to 240min, and at 392nm for 1440min. At the beginning of the reaction, there is irregular and a greater amount of nanoparticles surrounded by biomass from de aqueous extract; because the reaction is carried out at 60°C the biomass is degraded and presents more active sites (-OH), and not enough capping agents (-COOH), so the coarsening process takes place between the neighboring Ag-NPs, that is why the spectrum has lower intensity and widening of the SPR, this can be explained by the fluctuating behavior of the SPR during the reaction [34].

Polyphenolic compounds such as gallic acid, catechol, epicatechin and their derivatives, the two latter present in the *Camellia sinensis* extract, are known to form coordination complexes with heavy metals ions. The  $Pb^{2+}$  and  $Cu^{2+}$  preferentially bind to the carboxylic group in phenolic compounds [18,27,28]. A decrease in the intensity of the plasmon absorption at 400nm with time was observed (Figure 5a) when the Ag-NPs solution and the metal ions solutions were put in contact. This may be due to the appearance of agglomerates of the Ag-NPs with the metal ions provoked by the formation of the above mentioned complexes. These nanoparticles are stable at pH 5.27; in this pH range the carboxylic moieties of the capping biomolecules are present in the ionized form, which increase

the electronic interaction with the surface of the silver nanoparticle. The addition of  $Pb^{2+}$  and  $Cu^{2+}$  ions into the nanoparticles solution results also in a bathochromic shift in the plasmon absorption band as shown in Figure 5a, from 400 to 426nm and 403 to 412nm for lead and copper ions, respectively [23,25,28,35].

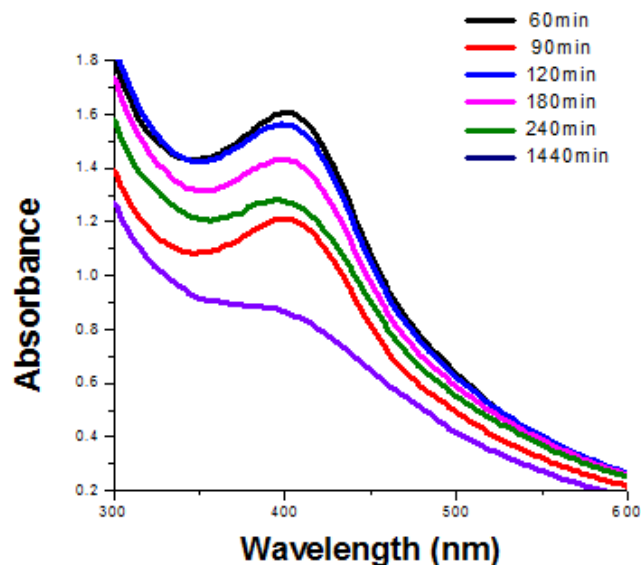


**Figure 4.** UV-Vis absorbance spectra of Ag-NPs at different times using 3mL of *Camellia sinensis* extract at 60°C.

These shifts in the plasmon absorption band and the visual color change (Figure 5a and 5b) can be likewise attributed to the formation of aggregates of Ag-NPs and the lead (II) and copper (II) ions [25-27,36]. It has been experimentally proven that the plasmon oscillation of metal nanoparticles couple to each other when they are in proximity. The new position of the resonance band is dependent on the number of nanoparticles together and their proximity [23,25,37]. These phenomena (shift of the plasmon resonance band induced by aggregation) have been successfully utilized for the colorimetric and plasmon detection of  $Pb^{2+}$  and  $Cu^{2+}$ .

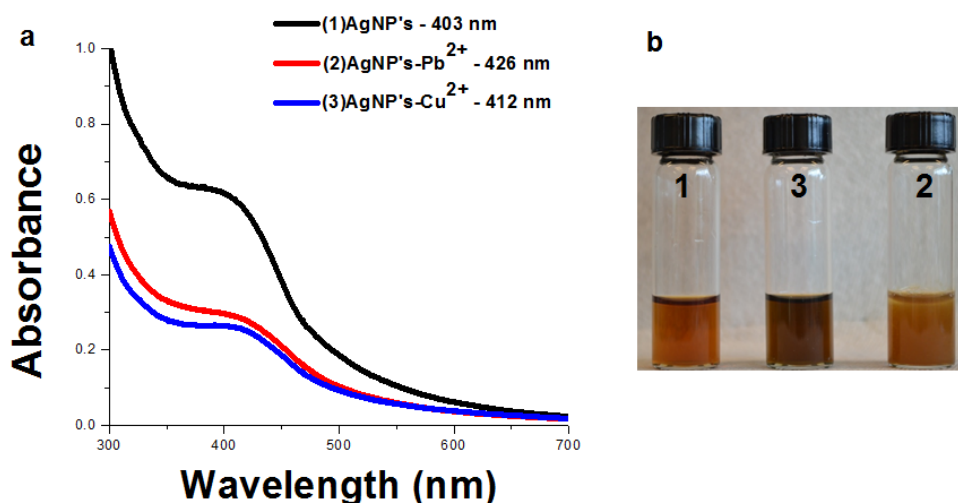


**Figure 5.** UV-Vis absorbance spectra of silver nanoparticles (1), silver nanoparticles upon adding  $\text{Pb}^{2+}$  ions (2) and silver nanoparticles upon adding  $\text{Cu}^{2+}$  ions (3), absorbances at  $\lambda_{\text{max}}$  are 400nm, 426nm and 412nm, respectively (a). Colorimetric response of silver nanoparticles and silver nanoparticles upon adding the metal ions ( $\text{Pb}^{2+}$  and  $\text{Cu}^{2+}$ ) (b).

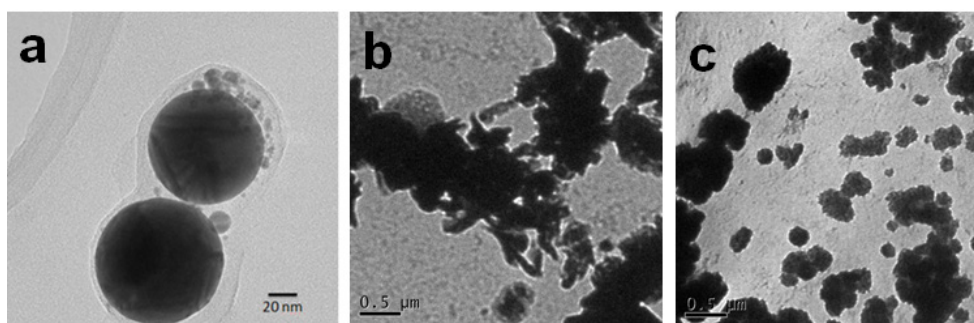


**Figure 6.** TEM images of Ag-NPs (a). TEM images of Ag-NPs after interaction with  $\text{Pb}^{2+}$  ions (b). TEM images of Ag-NPs after interaction with  $\text{Cu}^{2+}$  ions (c)

In order to confirm that the metal ions induce formation of Ag-NPs aggregates, TEM analyses were carried out. In the presence of  $\text{Pb}^{2+}$  and  $\text{Cu}^{2+}$  nanoparticles aggregates were observed, whereas, in the absence of the metal ions, the nanoparticles are surrounded by biomass as shown in Figure 6a. The thickness of the capping biomolecules is of about 4 to 12nm.

The complexation of the phenolic hydroxyl groups, from the biomolecules that are present as capping agents surrounding the nanoparticles, with the metal ions, can effectively bring nanoparticles closer to each other until coalescence process start and finally form the aggregates show in Figures 6b and 6c. This proximity induces the coupling of their plasmon oscillation, resulting in a bathochromic shift in the absorption band [23,25,38].

### 3.3.2. Sensibility Studies

To investigate the sensibility effect of the biogenic

Ag-NPs toward  $\text{Pb}^{2+}$  and  $\text{Cu}^{2+}$  metal ions, lead and cupric ions solutions with concentrations of  $10^{-3}$ ,  $10^{-4}$  and  $10^{-5}$  M were added to the Ag-NPs solution. These results are shown in Figure 7. The extent of the wavelength shift of the plasmon absorption depends on the concentration of the metal ions in the solution [23,27]. For example, the addition of  $10^{-3}$  M of  $\text{Pb}^{2+}$  resulted in a bathochromic shift of the plasmon absorption of 14 nm, from 400 to 414nm; however, with less concentration of the metal ions the shift diminish, from 400 to 411nm and from 400 to 408nm with concentrations of  $10^{-4}$  and  $10^{-5}$  M, respectively. When a  $\text{Cu}^{2+}$  solution with a concentration of  $10^{-3}$  M was utilized, the bathochromic shift of the plasmon absorption is of 12 nm, from 400 to 412nm. However, with less concentration of the metal ions the shift decreases, from 400 to 410nm and from 400 to 410nm with concentrations of  $10^{-4}$  and  $10^{-5}$ M, respectively.

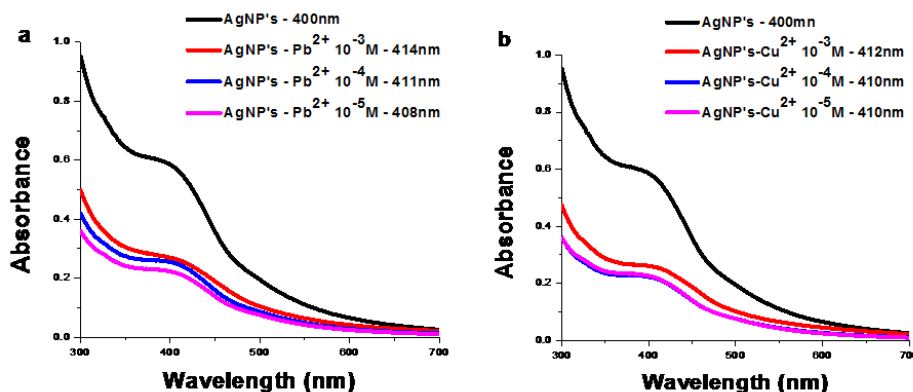


Figure 7. Absorption spectral changes of biogenic Ag-NPs upon addition of increasing concentrations ( $10^{-3}$  to  $10^{-5}$ M) of  $Pb^{2+}$ (a) and  $Cu^{2+}$  ions (b)

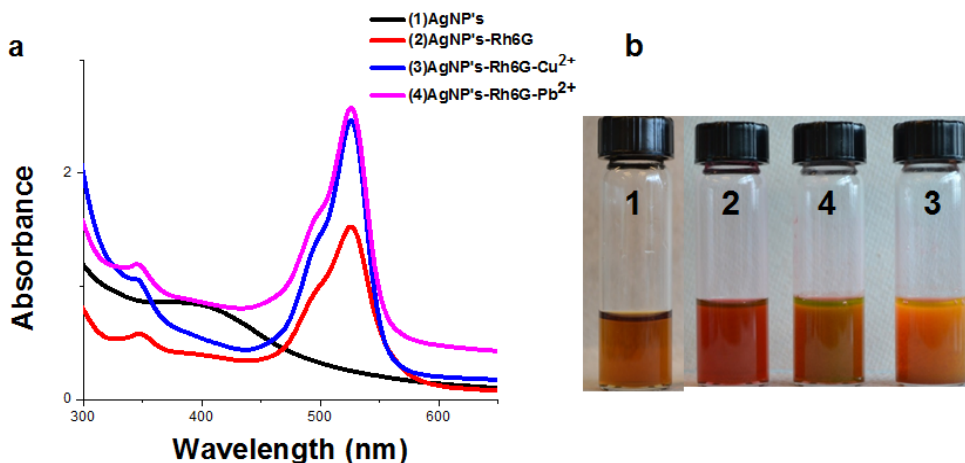


Figure 8. UV-Vis absorbance spectra of Ag-NPs (1), Ag-NPs-Rh6G (2), Ag-NPs-Rh6G-  $Cu^{2+}$  (3), Ag-NPs-Rh6G- $Pb^{2+}$  (4) (a). Photograph of Ag-NPs-Rh6G (2), Ag-NPs-Rh6G-  $Pb^{2+}$  (3), Ag-NPs-Rh6G- $Cu^{2+}$  (4) aqueous solutions (b).

### 3.3.3. Detection of Metal Ions Using Rh6G Dye

In this study, the combination of Ag-NPs-Rh6G dye act as probe for the detection of  $Pb^{2+}$  and  $Cu^{2+}$  ions. This heavy metal detection mechanism can occur via two steps; the first step involves the fixation of Rh6G molecules on the surface of the nanoparticles. The second step is the replacement of the Rh6G by the metal ions, the released of the dye acts as a visual colorimetric sensor; this methodology makes the eye-naked detection of  $Pb^{2+}$  and  $Cu^{2+}$  ions easier. Figure 8a exhibits UV-Vis absorption studies in aqueous solutions of bare Ag-NPs, Ag-NPs-Rh6G dye, AgNPs-Rh6G- $Cu^{2+}$  and AgNps-Rh6G- $Pb^{2+}$  Bare silver nanoparticles exhibited a single absorption SPR band at 400nm (Figure 8a, (1)), whereas, when Ag-NPs are in combination with Rh6G dye and lead and copper (II) ions, the corresponding spectra show double absorption maxima that can be attributed to the silver nanoparticles and Rh6G, respectively (Figure 8a (2,3,4)). The color of the Ag-NPs-Rh6G solution changes from orange to yellow when a copper (II) chloride solution, that provides  $Cu^{2+}$  ions, is added (Figure 8b (1,3)). Meanwhile, the addition of lead chloride, which provides  $Pb^{2+}$  ions, results in a green color solution with a light-brown precipitate (Figure 8b (1,2)).

### 3.3.4. Fluorescence Studies

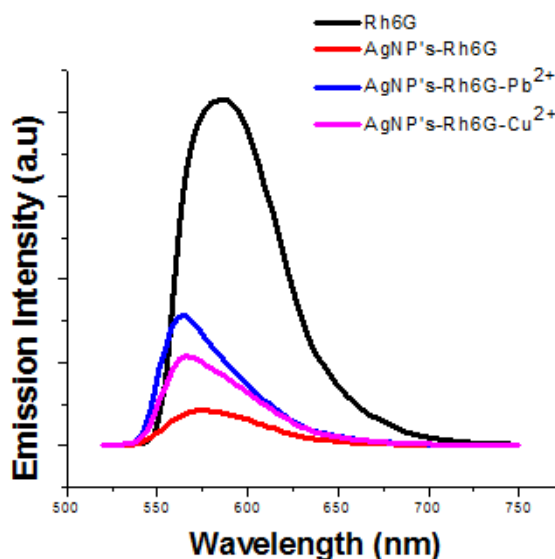


Figure 9. Fluorescence spectra of Rh6G, Ag-NPs-Rh6G, Ag-NPs-Rh6G- $Pb^{2+}$  and Ag-NPs-Rh6G- $Cu^{2+}$

Sensing studies were further evaluated using fluorescence spectrophotometry and the Rh6G fluorophore. The

attachment of Rh6G over the surface of Ag-NPs quenched the fluorescent emission of this dye through the fluorescence resonance energy transfer, as can be seen in Figure 9. This quenching confirms the interaction of Rh6G over the surface of nanoparticles. After the addition of the metal ions, the fluorescent emission is slightly restored (Figure 9).

The restoration of fluorescent emission ensures certain degree of detachment of the dye fluorophore from the nanoparticles surface provoked by the metal ions, and proves, thus, the sensing ability of these biogenic Ag-NPs produced by *Camellia sinensis* extract toward  $\text{Pb}^{2+}$  and  $\text{Cu}^{2+}$  ions [24,25].

## 4. Conclusions

A one-step green synthesis of Ag nanoparticles in water at  $60^\circ\text{C}$  was achieved by mixing  $\text{Ag}^+$  ions with  $\text{NH}_4\text{OH}$  and *Camellia sinensis* aqueous extract. The extract acts as a reducing and capping agent simultaneously. The biomediated Ag-NPs exhibited an FCC structure, revealed from TEM analysis. The bio-synthesized nanoparticles possess the ability to detect small quantities of  $\text{Pb}^{2+}$  and  $\text{Cu}^{2+}$  ions, resulting in a change of color solution (naked-eye) detection. In addition, the sensitivity Ag-NPs for the detection of  $\text{Pb}^{2+}$  and  $\text{Cu}^{2+}$  ions were probed by changes in the surface plasmon resonance with metal solution concentration, which is mainly attributed to the unique coordination behavior of the ions with the biomolecules surrounding the Ag-NPs. Moreover, with the aid of Rh6G dye in combination with Ag-NPs, it was possible to corroborate the facile detection of  $\text{Pb}^{2+}$  and  $\text{Cu}^{2+}$  ions both, naked-eye and by fluorescence spectroscopy, this latter detected as a restoration of the Ag-NPs-Rh6G solution quenched-emission signal.

## Acknowledgements

Financial support for this work was provided by the Universidad Autónoma del Estado de México, Grant 3688/2014/CIB. LESDH thanks to CONACYT (México) for doctorate scholarship.

## REFERENCES

- [1] B. Bhushan., Springer Handbook of Nanotechnology. Berlin: Bharat Bhushan. 2004.
- [2] M. Ramar, B. Manikandan, T. Raman et al., "Biosynthesis of silver nanoparticles using ethanolic petals extract of *Rosa indica* and characterization of its antibacterial, anticancer and anti-inflammatory activities," *Spectrochimica Acta Part A: Molecular and Biomolecular Spectroscopy*, vol.138, pp.120–129, 2015.
- [3] S. Murriello, D. Contier, M. Knobel., "Challenges of an exhibit on nanoscience and nanotechnology," *Science Communication*, vol.5, pp.1-11, 2006.
- [4] C. Noguez., "Optical properties of isolated and supported metal nanoparticles," *Optical Materials*, vol.27, pp.1204–1211, 2005.
- [5] C. Noguez., "Surface Plasmons on Metal Nanoparticles: The Influence of Shape and Physical Environment," *Journal of Physical Chemistry C*, vol.111, pp.3806-3819, 2006.
- [6] J. Lerne, H. Baida, C. Bonnet et al., "Size Dependence of the Surface Plasmon Resonance Damping in Metal Nanospheres," *Journal of Physical Chemistry Letters*, vol.1, pp.2922-2928, 2010.
- [7] F. Bisio, R.P. Zaccaria, R. Moroni et al., "Pushing the High-Energy Limit of Plasmonics," *ACS Nano*, vol.8, pp.9239–9247, 2014.
- [8] N.R. Jana, L. Gearheart, C. J. Murphy., "Wet chemical synthesis of silver nanorods and nanowires of controllable aspect ratio," *Chemical Communications*, pp.617-618, 2001.
- [9] S. Eliezer, N. Eliaz, E. Grossman et al., "Synthesis of nanoparticles with femtosecond laser pulses," *Physical Review B*, vol.69, pp.144119, 2004.
- [10] P.T. Anastas, M.M. Kirchoff., "Origins, Current Status, and Future Challenges of Green Chemistry," *Accounts of Chemical Research*, vol.35, no.9, pp.689-694, 2002.
- [11] A. Miri, M. Sarani, M.R. Bazaz et al., "Plant-mediated biosynthesis of silver nanoparticles using *Prosopis farcta* extract and its antibacterial properties," *Spectrochimica Acta Part A: Molecular and Biomolecular Spectroscopy*, vol.141, pp.287-291, 2015.
- [12] R. Bali, A.T. Harris., "Biogenic Synthesis of Au Nanoparticles Using Vascular Plants," *Industrial & Engineering Chemistry Research*, vol.49, no.24, pp.12762-12772, 2010.
- [13] S. Irvani, "Bacteria in Nanoparticle Synthesis: Current Status and Future Prospects," *International Scholarly Research Notices*, Vol.2014, pp.18, 2014.
- [14] N. Kannan, S. Subbalaxmi., "Biogenesis of nanoparticles – a current perspective," *Reviews on advanced materials science*, vol.27, pp.99-114, 2011.
- [15] K.B. Narayanan, N. Sakthivel., "Green synthesis of biogenic metal nanoparticles by terrestrial and aquatic phototrophic and heterotrophic eukaryotes and biocompatible agents," *Advances in Colloid and Interface Science*, vol.169, pp.59–79, 2011.
- [16] A.K. Jha, K. Prasad, K. Prasad et al., "Plant system: Nature's nanofactory," *Colloids and Surfaces B: Biointerfaces*, vol.73, no.2, pp.219-223, 2009.
- [17] G. Zhan, J. Huang, L. Lin, et al., "Synthesis of gold nanoparticles by *Cacumen Platycladi* leaf extract and its simulated solution: toward the plant-mediated biosynthetic mechanism," *Journal of Nanoparticle Research*, vol.13, pp.4957-4968, 2011.
- [18] T.M. Rababah, N.S. Hettiarachchy, R. Hora., "Total phenolics and antioxidant activities of fenugreek, green tea, black tea, grape seed, ginger, rosemary, gotu kola, and ginkgo

- extracts, vitamin E, and tert-butylhydroquinone,” *Journal of Agricultural and Food Chemistry*, vol.52, no.16, pp.5183-5186, 2004.
- [19] N. A. Begum, S. Mondal, S. Basu, et al., “Biogenic synthesis of Au and Ag nanoparticles using aqueous solutions of Black Tea leaf extracts,” *Colloids Surf B Biointerfaces*, vol.71, no.1, pp.11-118, 2009.
- [20] L.E. Silva De Hoyos, V. Sánchez Mendieta, A.R. Vilchis Nestor, et. Al., “Silver nanoparticles biosynthesized using *Opuntia ficus aqueous extract*,” *Superficies Vacío*, vol.25, no.1, pp.31-35, 2012.
- [21] S.E. Lohse, C.J. Murphy, “Applications of Colloidal Inorganic Nanoparticles: From Medicine to Energy,” *Journal of the American Chemical Society*, vol.134, no.38, pp.15607-15620, 2012.
- [22] B. Saha, J. Bhattacharya, A. Mukherjee, et al., “In Vitro Structural and Functional Evaluation of Gold Nanoparticles Conjugated Antibiotics,” *Nanoscale Research Letters*, vol.2, no.12, pp.614-622, 2007.
- [23] K. Yoosaf, B.I. Ipe, C.H. Suresh, et al., “In Situ Synthesis of Metal Nanoparticles and Selective Naked-Eye Detection of Lead Ions from Aqueous Media,” *Journal of Physical Chemistry A*, vol.111, no.34, pp.12839-12847, 2007.
- [24] M. Annadhasan, T. Muthukumarasamyvel, V. R. Sankar Babu, et al., “Green Synthesized Silver and Gold Nanoparticles for Colorimetric Detection of  $Hg^{2+}$ ,  $Pb^{2+}$ , and  $Mn^{2+}$  in Aqueous Medium,” *ACS Sustainable Chemistry & Engineering*, vol.2, pp.887-896, 2014.
- [25] J. Langer, S.M. Novikov, L.M Liz-Marzán., “Sensing using plasmonic nanostructures and nanoparticles,” *Nanotechnology*, vol.26, no.32, pp.322001, 2015.
- [26] K.S. Lee, M.A. El-Sayed., “Gold and Silver Nanoparticles in Sensing and Imaging: Sensitivity of Plasmon Response to Size, Shape, and Metal Composition,” *Journal of Physical Chemistry B*, vol.110, no.39, pp.19220-19225, 2006.
- [27] C. J. Kirubakaran, D. Kalpana, Y.S. Lee, et al., “Biomediated Silver Nanoparticles for the Highly Selective Copper(II) Ion Sensor Applications,” *Industrial & Engineering Chemistry Research*, vol.51, no.21, pp.7441-7446, 2012.
- [28] C. Wang, C. Yu., “Detection of chemical pollutants in water using gold nanoparticles as sensors: a review,” *Industrial & Engineering Chemistry Research*, vol.32, no.1, pp.1-14, 2013.
- [29] L. Polavarapu, L.M. Liz-Marzán., “Towards low-cost flexible substrates for nanoplasmonic sensing,” *Physical Chemistry Chemical Physics*, vol. 15, pp. 5288-5300, 2013.
- [30] K. Saha, S.S. Agasti, C. Kim, et al., “Gold nanoparticles in chemical and biological sensing,” *Chemical Reviews*, vol. 112, no. 5, pp. 2739-2779, 2012.
- [31] L. Polavarapu, J. Pérez-Juste, L.M. Liz-Marzán, et al., “Optical sensing of biological, chemical and ionic species through aggregation of plasmonic nanoparticles,” *Journal of Materials Chemistry C*, vol.2, pp.7460-7476, 2014.
- [32] J.L. Gardea-Torresdey, E. Gomez, J.R. Peralta-Videa, et al., “Alfalfa Sprouts: A Natural Source for the Synthesis of Silver Nanoparticles,” *Langmuir*, vol.19, no.4, pp.1357-1361, 2003.
- [33] Amendola, O.M. Bakr, F. Stellacci., “A Study of the Surface Plasmon Resonance of Silver Nanoparticles by the Discrete Dipole Approximation Method: Effect of Shape, Size, Structure, and Assembly,” *Plasmonics*, vol.5, no.1, pp.85-97, 2010.
- [34] S. E. Hunyadi Murph, C. J. Murphy, A. Leach, et. al., “A Possible Oriented Attachment Growth Mechanism for Silver Nanowire Formation,” *Crystal Growth & Design*, vol.15, no.4, pp.1968-1974, 2015.
- [35] N. Ding, H. Zhao, W. Peng, et al., “A simple colorimetric sensor based on anti-aggregation of gold nanoparticles for  $Hg^{2+}$  detection,” *Colloid Surface A: Physicochemical and Engineering Aspects*, vol.395, pp. 161- 167, 2012.
- [36] M. Li, H. Gou, I. Al-Ogaidi, et al., “Nanostructured Sensors for Detection of Heavy Metals: A Review,” *ACS Sustainable Chemistry & Engineering*, vol.1, pp.713-723, 2013.
- [37] T. Lou, Z. Chen, Y. Wang, et al., “Blue-to-Red Colorimetric Sensing Strategy for  $Hg^{2+}$  and  $Ag^{+}$  via Redox-Regulated Surface Chemistry of Gold Nanoparticles,” *ACS Applied Materials & Interfaces*, vol.3, pp.1568-15730, 2011.
- [38] V.V. Kumar, S.P. Anthony., “Silver nanoparticles based selective colorimetric sensor for  $Cd^{2+}$ ,  $Hg^{2+}$  and  $Pb^{2+}$  ions: Tuning sensitivity and selectivity using co-stabilizing agents,” *Sensors and Actuators B: Chemical*, vol.191, pp.31-36, 2014.